Use of Adaptive Methods in Premixed Combustion

This paper investigates the application of spatially adaptive numerical methods in the solution of one-dimensional premixed combustion problems. The selection of grid points by equidistribution of positive weight functions across consecutive mesh intervals is considered. The method is applied in the solution of a steady premixed laminar flame problem and a time-dependent freely propagating flame problem. The adaptive numerical results are compared with corresponding equispaced calculations.

M. D. Smooke
Department of Mechanical Engineering
Yale University
New Haven, CT 06520

Introduction

The solution of combustion problems by numerical methods can provide the researcher with information that is not often obtainable from experiment. For example, in the calculation of premixed flame structure, the kineticist can investigate the important elementary reaction paths in simple fuels (Miller et al., 1982, 1983). For flames such as ozone-oxygen and hydrogen-oxygen, the calculations can be performed on moderate size computers with several hundred equispaced grid points. However, the solution of more complicated systems (e.g., methane, ammonia, and acetylene) on equispaced grids can become prohibitively expensive on even the largest scientific computers. In these problems we typically desire solution profiles to as many as 40 chemical species with over 100 chemical reactions. The situation becomes even worse if solutions are desired in two dimensions (Smooke and Koszykowski, 1984). In such cases all but the very simplest of flames are computationally infeasible—the larger problems will not even fit in the central memory of most machines.

Given such limitations, the combustion scientist is faced with the dilemma of either reducing the number of species in the reaction mechanisms of the more complex fuels or of utilizing numerical algorithms that place grid points adaptively in the regions where they are needed—large numbers of points where the species change rapidly and smaller numbers of points in the slowly varying regions. Such methods are able to conserve the number of grid points used in a calculation without compromising accuracy. In designing an adaptive algorithm, the researcher often requires the variation of a positive weight function (e.g., local truncation error) to be constant (equidistributed) from one spatial interval to another. Aside from the choice of whether finite-difference or finite-element spatial discretizations are employed, many of the adaptive methods appearing in the literature differ primarily in the choice of the weight functions and whether they depend explicitly or implicitly upon the solution.

Adaptive methods have been developed for both steady-state and time-dependent problems. For example, in the solution of two-point boundary value problems, White (1979) has developed a procedure that equidistributes the arclength of the solution, and in the method considered by Pereyra and Sewell (1975), the local truncation error is equidistributed among consecutive mesh intervals (see also Ascher et al., 1979). Several adaptive approaches for solving mixed initial-boundary value problems have also appeared recently in the literature. We mention the finite-element methods of Miller and Miller (1981) and Davis and Flaherty (1982) as well as the arclength method of White (1982). Variations of these methods have been used with increased frequency in the solution of problems in fluid flow, heat and mass transfer, and combustion. For example, Smooke (1982) and Smooke et al. (1983, 1985) have applied such methods in the solution of one-dimensional laminar premixed and counterflow diffusion flame problems. They have been used by Tscharnuter and Winkler (1979) in self-gravitating gas flow calculations, and Dwyer et al. (1980, 1982) have applied them in heat transfer calculations. Other applications include work by Harten and Hyman (1983), Larrouturou (1985), and Sermange (1985).

Our goal in this paper is to illustrate the effectiveness of adaptive computational procedures in a specific application—premixed combustion. We apply one-dimensional spatially adaptive methods in the calculation of the structure of a steady-state and a time-dependent premixed laminar flame. In both cases we compare the efficiency of the adaptive calculations with corresponding equispaced results. In the next section we introduce some preliminary material. In succeeding sections we discuss the concept of equidistribution in the adaptive selection of grid points, and then numerical results.

Preliminaries

In this paper spatially adaptive grid methods will be applied to two premixed flame problems. In each case, the governing equations can be written in terms of a canonical mathematical problem: a two-point boundary value problem and a mixed initial-boundary value problem. The steady-state problem can be written in the form

$$f(x, u, u_x, u_{xx}) = 0, \quad a < x < b, \tag{1a}$$

$$g_1[a, u(a), u_x(a)] = 0, \tag{1b}$$

$$g_2[b, u(b), u_x(b)] = 0, \tag{1c}$$

and the time-dependent problem is given by

$$u_t = f(x, t, u, u_x, u_{xx}), \quad a < x < b, \quad t > 0, \tag{2a}$$

$$g_1[a, t, u(a), u_x(a)] = 0, \quad t > 0, \tag{2b}$$

$$g_2[b, t, u(b), u_x(b)] = 0, \quad t > 0, \tag{2c}$$

$$u(x, 0) = r(x), \quad a < x < b, \tag{2d}$$

where u, f, g_1, g_2, and r are N vectors.

Difference formulation

Problems in combustion and heat and mass transfer can often be written in the form of either Eq. 1 or Eq. 2 (Peters and Warnatz, 1982). Many of these problems are sufficiently complex that analytical solutions cannot be obtained. As a result, numerical methods must be used. For the steady-state case, solution of Eq. 1 is sought on a discrete mesh $\mathcal{M}$

$$\mathcal{M} = \{a = x_0 < x_1 < \cdots < x_M = b\}, \tag{3}$$

where $h_j = x_j - x_{j-1}, j = 1, 2, \ldots, M$. Inherent to the solution procedure is the discretization of the spatial derivative operators by finite-difference expressions. For example, second-order spatial derivatives can be approximated by

$$\frac{\partial}{\partial x}\left[a(x)\frac{\partial g}{\partial x}\right]_{x_j} \approx \partial^2(a_j g_j) = \left(\frac{2}{x_{j+1} - x_{j-1}}\right)(a_{j+1/2}\partial g_{j+1} - a_{j-1/2}\partial g_j), \tag{4}$$

where we define $g_j = g(x_j), j = 0, 1, \ldots, M$, and

$$g_{j+1/2} = \frac{(g_{j+1} + g_j)}{2}, \quad j = 0, 1, \ldots, M - 1, \tag{5}$$

$$\partial g_{j+1} = \frac{(g_{j+1} - g_j)}{h_{j+1}}, \quad j = 0, 1, \ldots, M - 1, \tag{6}$$

with corresponding expressions for first derivatives.

For time-dependent problems we start from the initial point $t^0 = 0$ and seek a numerical solution of Eq. 2 at time levels $0 = t^0 < t^1 < t^2 < \cdots < t^J = \mathcal{T}$, for some finite time $\mathcal{T}$ on the mesh $\mathcal{M}^{n+1}$ where

$$\mathcal{M}^{n+1} = \{a = x_0^{n+1} < x_1^{n+1} < \cdots < x_{M^{n+1}}^{n+1} = b\}. \tag{7}$$

The superscript on the mesh accounts for the fact that in a time-dependent problem the number as well as the location of the grid points may change from one time level to another. Discretization of the spatial operators is accomplished as in Eq. 4. The time derivatives must also be discretized and, for reasons of numerical stability as well as computational efficiency, we use backward-differentiation formulas. If we define $g^n(x) = g(x, t^n), n = 0, 1, 2, \ldots, J$, then upon employing a backward-Euler time-difference approximation and neglecting the time-discretization error, we have the following semidiscrete approximation to Eq. 2

$$f(x, t^{n+1}, \tilde{u}^{n+1}, \tilde{u}_x^{n+1}, \tilde{u}_{xx}^{n+1}) - \frac{\tilde{u}^{n+1}}{\tau^{n+1}} = -\frac{\tilde{u}^n}{\tau^{n+1}}, \tag{8a}$$

$$g_1[a, t^{n+1}, \tilde{u}^{n+1}(a), \tilde{u}_x^{n+1}(a)] = 0, \tag{8b}$$

$$g_2[b, t^{n+1}, \tilde{u}^{n+1}(b), \tilde{u}_x^{n+1}(b)] = 0, \tag{8c}$$

$$\tilde{u}^0(x) = r(x), \tag{8d}$$

for $n = 0, 1, 2, \ldots, J - 1$, where the time step $\tau^{n+1} = t^{n+1} - t^n$ and where the change of notation from u to $\tilde{u}$ recognizes the fact that the solution of Eq. 8 is in general different from the solution of Eq. 2. We observe that solution of the original mixed initial-boundary value problem has been reduced to solving an inhomogeneous nonlinear two-point boundary-value problem at each time level. Hence the problems in Eq. 8 can be solved by techniques similar to those used in solving Eq. 1.

Newton's method

If we replace the spatial operators in Eqs. 1 and 8 by difference expressions, we convert the problem of finding an analytic solution of the original equations into one of finding an approximation to it at each point of the mesh $\mathcal{M}$ or $\mathcal{M}^{n+1}$. If we omit the time level superscript, then the discrete approximation of the original differential equations can be written in the residual form

$$F(V) = 0, \tag{9}$$

where the vector $V = (v_{i,j}), i = 1, 2, \ldots, N$ and $j = 1, 2, \ldots, M$, represents the solution at each point of the grid. Solution of the nonlinear equations in Eq. 9 often proceeds by application of a variation of Newton's method (Ascher et al., 1979; White, 1979, 1982; Smooke, 1982, 1983; Smooke and Koszykowski, 1986). For an initial solution estimate that is sufficiently close to the solution, we perform the following iteration

$$J(V_k)(V_{k+1} - V_k) = -\lambda_k F(V_k), \quad k = 0, 1, \ldots, \tag{10}$$

where V_k denotes the kth solution iterate, λ_k the kth damping parameter ($0 < \lambda \leq 1$) (Deuflhard, 1974), and $J(V_k) = \partial F(V_k)/\partial V$ the Jacobian matrix. At each iteration a system of linear equations is solved for corrections to the previous solution

vector. The iteration is terminated when $\|V_{k+1} - V_k\|$ is sufficiently small.

Once a solution of Eq. 9 has been obtained for either the steady state case or for one time level of the transient problem, the question arises as to whether the grid is sufficiently dense in the high-activity regions to resolve the solution accurately. In the next section we discuss the concept of equidistribution as a method to place grid points systematically in the high-activity regions.

Equidistribution and the Adaptive Selection of Grid Points

Differential equations that model the behavior of physical systems often give rise to solutions that exhibit rapid variation over small spatial domains. For example, the temperature of a premixed laminar flame several centimeters in length can rise two thousand degrees in only one or two millimeters (Miller et al., 1982, 1983). These problems are said to exhibit regions of high spatial activity (sharp peaks and steep fronts). For reasons of accuracy, it is important to resolve these high-activity domains. However, from the point of view of efficiency, the use of an equispaced grid can require an excessively large number of points. Even if the problem can be fit in core, the CPU time can make the calculation computationally impractical. As an example, consider the somewhat contrived problem of a piecewise linear temperature rise in a premixed laminar flame of length 5 cm. Suppose that the temperature increases from 300 to 400 K over the domain $0.0 \le x \le 0.9$ cm. For $0.9 \le x \le 1.0$ cm it increases from 400 to 2,000 K and for $1.0 \le x \le 5.0$ cm it rises to 2,100 K. In addition, suppose accuracy considerations require that we resolve the temperature to within 100 K between consecutive mesh points. A simple calculation shows that if an equispaced grid were used over the entire domain, we would need 800 grid points. However, if an adaptive grid were used we would need less than 20 points, a factor of roughly 40 less. Hence, providing that the cost of selecting the grid points adaptively is not too expensive, we can obtain considerable savings in CPU time and we can solve larger systems in core than if equispaced methods are used.

In designing an adaptive algorithm we want to select the location of the grid points so that we attain a high degree of accuracy (ideally a small global error) with a small number of points. For example, one could place grid points in regions where the discretization error was high (Pereyra and Sewell, 1975) or where the solution changed most rapidly (Pearson, 1968). In addition, we also desire the accuracy level to be comparable from one subinterval to another. The concept of equalizing changes in some property of a differential operator or the solution of a differential equation over consecutive subintervals is called equidistribution. Many of the methods that have been used to obtain adaptive grid spacings for two-point boundary value problems can be interpreted in terms of equidistributing a positive weight function on a given interval (e.g., Kautsky and Nichols, 1980). Essentially, one attempts to determine a mesh $\mathcal{M}$ such that the weight function achieves the same variation over each subinterval. For a discussion of various equidistribution methods see Russell (1979).

More precisely, we say that the mesh $\mathcal{M}$ is equidistributed on $[a, b]$ with respect to the nonnegative function w and the constant C if

$$\int_{x_j}^{x_{j+1}} w\,dx = C, \quad j = 0, 1, \ldots, M-1. \tag{11}$$

A method we have found to be quite effective in combustion problems, and at the same time easy to implement, is the equidistribution of the difference in the components of the solution and its gradient over consecutive intervals. If we denote the vector $u = [u_1, u_2, \ldots, u_N]^T$, we seek to obtain a mesh $\mathcal{M}$ such that

$$\int_{x_j}^{x_{j+1}} \left|\frac{du_i}{dx}\right| dx \le \delta \left|\max_{a\le x\le b} u_i - \min_{a\le x\le b} u_i\right|$$
$$j = 0, 1, \ldots, M-1; i = 1, 2, \ldots, N \tag{12}$$

and

$$\int_{x_j}^{x_{j+1}} \left|\frac{d^2u_i}{dx^2}\right| dx \le \gamma \left|\max_{a\le x\le b} \frac{du_i}{dx} - \min_{a\le x\le b} \frac{du_i}{dx}\right|$$
$$j = 1, 2, \ldots, M-1; i = 1, 2, \ldots, N \tag{13}$$

where δ and γ are small numbers less than one and the values of $\max u_i$, $\min u_i$, $\max du_i/dx$, and $\min du_i/dx$ are estimated from a numerical solution on a previously determined mesh.

In the implementation of the adaptive mesh algorithm, we first solve the boundary value problems in Eq. 9 on a given mesh. The maximum and minimum values of u_i and du_i/dx are then obtained. We next test the inequalities in Eqs. 12 and 13 for each of the N-dependent solution components at the nodes of the mesh. If either of the inequalities is not satisfied, a grid point is inserted at the midpoint of the interval in question. The numerical solution from the original grid is then interpolated onto the new mesh and the result serves as an initial solution estimate for Newton's method on this finer grid. The process continues until the inequalities in Eqs. 12 and 13 are satisfied.

For steady state problems at least one Jacobian matrix is formed and factored on each grid. This procedure can also be used at each time level for time-dependent problems. However, the formation and factorization of one or more Jacobians at every time step can become computationally expensive. It is also important to point out that the high-activity regions in time-dependent problems can move as the solution is advanced. In addition, new high-activity regions can appear and old high-activity regions can disappear. If the high-activity regions increase, the number of grid points should adjust to maintain a fixed level of accuracy. By applying the boundary value problem mesh selection procedure described above, the number of nodes will adjust at each time level to satisfy Eqs. 12 and 13. Grid points will be inserted on increasingly finer grids based upon whether the local values of the integrals are greater than the corresponding righthand sides. In principle, the number of points at level n can differ from the number of points at level $n + 1$. However, if the high-activity regions propagate without an increase or decrease in spatial activity, a fixed number of moving grid points can often maintain a given level of accuracy.

In a fixed-node method the dimension of the Jacobian does not change. Its factorization can be stored and it can be used for

several time steps. Hence, the cost of propagating the solution will, in general, be less than if the variable-node method were used (increasing the size of the system requires the formation and factorization of a new Jacobian). The equidistribution procedure in Eqs. 12 and 13 can be modified to accommodate a fixed number of nodes. If the integrals in Eqs. 12 and 13 are computed first over the entire domain and if these quantities are then divided by the specified number of subintervals, we can obtain a value of the equidistribution constant C. This represents the desired change in the solution and its derivative from one point to another. If we next evaluate the integrals one subinterval at a time and if we determine the interval in which the cumulated value of the integrals becomes greater than C, the location of the first grid point can be determined by applying an inverse interpolation algorithm. This process can then be restarted and the integrals evaluated until they again become larger than C. In this way we can determine the location of each of the remaining interior grid points. Such a procedure has the advantage that, since the size of the Jacobian does not change from one time level to another, it can be used for several time steps. It can, however, produce grid point locations that differ from one time to another. This requires an interpolation strategy.

We observe that solution of the boundary value problem in Eq. 8 at time level $n + 1$ requires a knowledge of the solution at time level n at the points of the mesh $\mathcal{M}^{n+1}$. If the same spatial grid were used for the entire calculation—at time levels t^0, t^1, ..., t^J—we would have solution values available at the proper mesh points. The physical locations of the grid points at one time level would be identical to the locations of the points at any other. However, since we employ an inverse interpolation procedure in the time-dependent case, it is likely that the location of the grid will change from one time step to another. In such cases we interpolate solution values from the previous time step to obtain solution information corresponding to the location of the grid points at the current time. (We point out that, if a finite-element solver had been used, the interpolation problem would disappear since a continuous representation of the solution would be available).

In our finite-difference method we must be able to relate a given grid point at level $n + 1$ with the same physical point at level n. This procedure is discussed in detail in Smooke and Koszykowski (1986). For our purposes, suppose the grid points at time levels $n + 1$ and n are given as in Figure 1. We see that the point at level $n + 1$ does not coincide with any point from level n. We assume, however, that we can bound the point x_j^{n+1} above and below by two points from the nth level, say x_k^n and x_{k+1}^n. To obtain the discrete solution v_j^n we form

$$v_j^n = v_k^n + \left(\frac{v_{k+1}^n - v_k^n}{x_{k+1}^n - x_k^n}\right)(x_j^{n+1} - x_k^n), \tag{14}$$

or a corresponding expression if x_j^{n+1} is closer to x_{k+1}^n. An additional spatial discretization error is introduced into the finite-difference algorithm as a result of the interpolation procedure used in Eq. 14. This error influences the way the time steps are chosen.

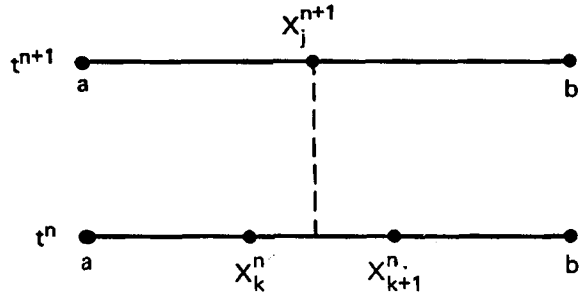

Figure 1. Grid points at time levels n and $n + 1$.
Physical location of x_j^{n+1} does not coincide with either x_k^n or x_{k+1}^n.

Numerical Results

In this section we illustrate application of the adaptive methods discussed in the previous section in the solution of two premixed laminar flames. In both cases we compare the results of several equispaced calculations and an adaptive calculation. In particular, we focus on the difference in propagation velocities and on the resolution of the various solution components. All of the computations were performed on a CRAY-1S computer.

Problem 1

The first problem we consider is an adiabatic, atmospheric pressure, hydrogen-air flame. The reaction mechanism for this flame (see Appendix) is well understood, so we can eliminate the effect of variations in the reactions on our results.

We compare the effects of using several equispaced grids and an adaptive grid in the calculation of adiabatic flame speeds. We also illustrate the effects of using these grids on the resolution of the flame's minor species.

Our goal in adiabatic premixed flame calculations is to predict:

1. The mass fraction and temperature profiles as functions of the independent spatial coordinate.
2. The mass flow rate or flame speed.

We point out that the laminar flame speed is a convenient, and often-measured global parameter that is used to characterize combustion of premixed fuel-oxidizer mixtures. The ability to predict the flame speed correctly is important to the combustion chemist who is attempting to understand the detailed chemical kinetic processes in flames.

In the flame model we consider (Smooke et al., 1983), we assume that the flame is one-dimensional and that viscous effects, radiative heat transfer, body forces, and the diffusion of heat due to concentration gradients (Dufour effect) are negligible. Hence, the governing equations can be written

$$\dot{M} = \rho v = \text{constant}, \tag{15}$$

$$\dot{M}\frac{dY_k}{dx} = -\frac{d}{dx}(\rho Y_k V_k) + \dot{\omega}_k W_k, \quad k = 1, 2, \ldots, K, \tag{16}$$

$$\dot{M}\frac{dT}{dx} = \frac{1}{c_p}\frac{d}{dx}\left(\lambda\frac{dT}{dx}\right) - \frac{1}{c_p}\sum_{k=1}^{K}\rho Y_k V_k c_{p_k}\frac{dT}{dx} - \frac{1}{c_p}\sum_{k=1}^{K}\dot{\omega}_k h_k W_k, \tag{17}$$

$$\frac{d\dot{M}}{dx} = 0, \tag{18}$$

$$\rho = \frac{p\overline{W}}{RT}. \tag{19}$$

In these equations x denotes the independent spatial coordinate fixed to the flame; $\dot{M}$, the mass flow rate; T, the temperature; Y_k, the mass fraction of the kth species; p, the pressure; v, the velocity of the fluid mixture; ρ, the mass density; W_k, the molecular weight of the kth species; $\overline{W}$, the mean molecular weight of the mixture; R, the universal gas constant; λ, the thermal conductivity of the mixture; c_p, the constant pressure heat capacity of the mixture; c_{pk}, the constant pressure heat capacity of the kth species; $\dot{\omega}_k$, the molar rate of production of the kth species per unit volume; h_k, the specific enthalpy of the kth species; and V_k, the diffusion velocity of the kth species. The diffusion velocity incorporates Fickian diffusion and thermal diffusion effects. The detailed form of the chemical production rates and the transport coefficients can be found in Kee et al. (1980, 1983).

The problem is posed physically on the infinite domain $-\infty \le x \le \infty$. For computational purposes we solve the equations on the finite domain $0 \le x \le L$ where L is chosen large enough to insure that the flame speed and the temperature and species profiles are not affected significantly by the choice of L. The boundary conditions can be written in the form

$$T(0) = T_0, \tag{20}$$

$$\epsilon_k(0) = Y_{k_0}, \quad k = 1, 2, \ldots, K, \tag{21}$$

and at $x = L$,

$$\frac{dT}{dx}(L) = 0, \tag{22}$$

$$\frac{dY_k}{dx}(L) = 0, \quad k = 1, 2, \ldots, K, \tag{23}$$

where the mass flux fraction of the kth species is defined as,

$$\epsilon_k = Y_k + \frac{\rho Y_k V_k}{\dot{M}}, \quad k = 1, 2, \ldots, K. \tag{24}$$

To complete the specification of the problem we need an additional boundary condition for the flame speed equation, Eq. 18. The particular choice of the extra boundary condition is somewhat arbitrary. Our experience has shown that the solution procedure is most sensitive to variations in the temperature; as a result, we choose to fix the temperature at an interior grid point. We specify

$$T(x_f) = T_f, \tag{25}$$

where x_f is a specified interior grid point and T_f is the specified temperature at this point. Values of x_f and T_f must be chosen such that the flame sits sufficiently far from the boundary so that dT/dx and dY_k/dx are vanishingly small at $x = 0$ and are consistent with the boundary conditions for the infinite domain. We point out that if the derivatives of T and Y_k are not small enough, the length of the computational domain can be increased easily with the addition of only a few grid points. The adaptive gridding procedure places the largest mesh intervals in the asymptotic region. Doubling the length of the domain ordinarily requires only one or two additional mesh intervals.

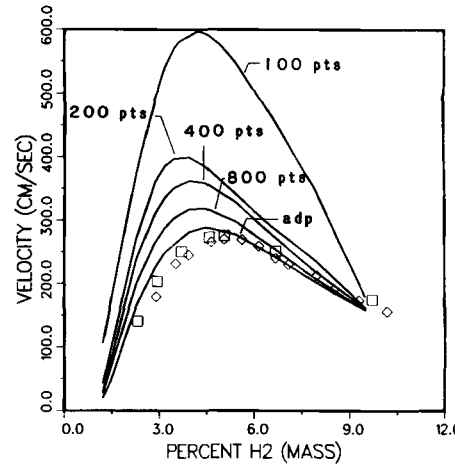

Figure 2. Comparison of computed atmospheric pressure, hydrogen-air flame speeds with data compilation of Dixon-Lewis (1979).

In calculating adiabatic flame speeds we first solve Eqs. 15–25 for a given fuel-oxidizer ratio (e.g., stoichiometric conditions). A continuation procedure is then used to vary the percentage of fuel in the reacting mixture. The solution for one value of the fuel-oxidizer ratio provides an excellent starting estimate for another problem with a different ratio. The adaptive gridding procedure also has the ability to adjust the number of grid points needed to maintain a specific degree of accuracy. If the location of the flame zone shifts as the fuel-oxidizer ratio is adjusted, the mesh adjusts itself accordingly.

In all of the flame speed calculations we began the continuation procedure on an atmospheric pressure, stoichiometric, hydrogen-air flame. The fuel-oxidizer ratio was then changed gradually in both the rich and the lean directions to obtain flame speeds for various percentages of hydrogen. We performed calculations on equispaced grids consisting of 100, 200, 400, and 800 points and on an adaptive grid in which the nodes varied between 39 and 45 points. The length of the computational

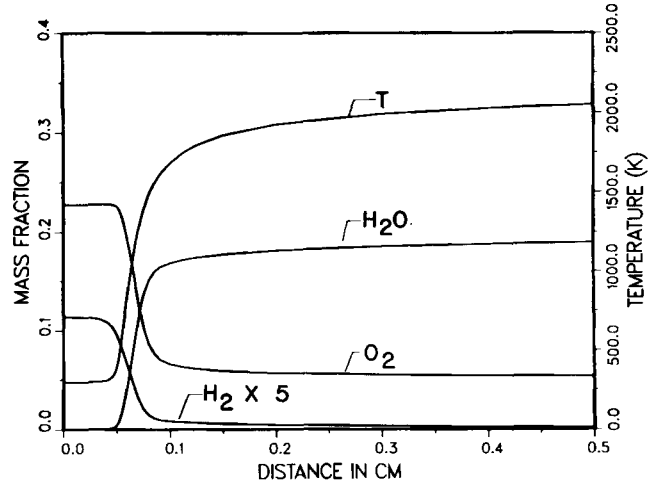

Figure 3. Temperature and major species profiles for a lean hydrogen-air flame.

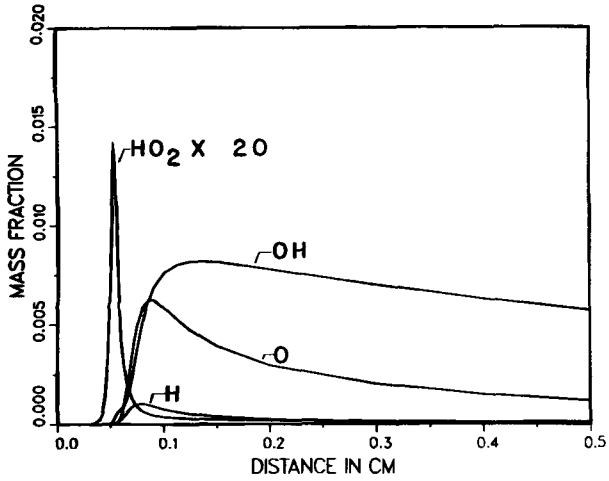

Figure 4. Minor species profiles for a lean hydrogen-air flame.

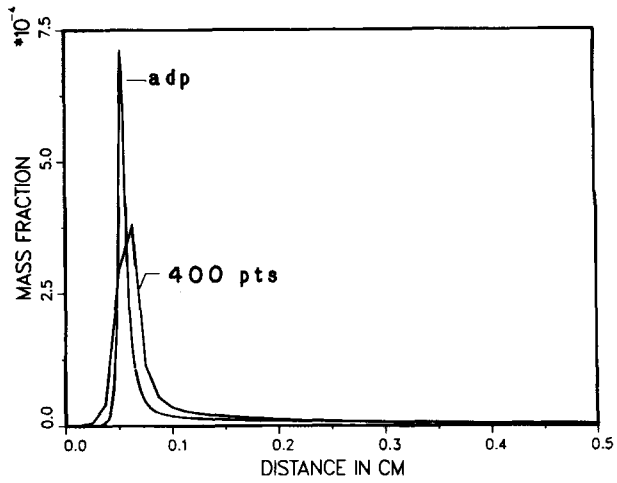

Figure 6. Comparison of HO_2 profile for adaptive calculation with 400-point equispaced result.

domain was 5 cm, and in all of the calculations $x_f = 0.05$ cm and $T_f = 400$ K.

In Figure 2 we illustrate a comparison of our results with some of the flame speed data compiled by Dixon-Lewis (1979). (The kinks in the flame speed profiles result from the number of continuation steps used in going from lean to rich conditions. More continuation steps would produce smoother profiles.) We observe immediately the extremely high flame speeds for the equispaced grids consisting of 100 and 200 points. In fact, it is not until we use 800 equispaced points that we obtain flame speeds that are within 10–15% of the adaptive calculations. The results indicate clearly that more than 800 points are needed to obtain results comparable to the adaptive calculation.

In Figures 3 and 4 we illustrate the adaptive temperature and species profiles for a lean (2.28% H_2) hydrogen-air flame. From the results we observe that the HO_2 concentration exhibits a very sharp profile—a good example of high spatial activity. The adaptive calculation concentrated 21 of its 40 points in the region where the mass fraction of HO_2 was greater than 10% of its peak value. In Figures 5, 6, and 7 we compare the equispaced HO_2 profiles with the corresponding adaptive calculation. We observe immediately the lack of resolution and the difference among the peak heights of the equispaced profiles and the adaptive calculation. Again, it is not until 800 points are used that we obtain peak heights and half-widths within 15–20% of the adaptive results. In fact, based upon the minimum mesh spacing used in the adaptive calculation, we anticipate that as many as 1,200 equispaced points are needed to give results comparable to the adaptive calculation. In addition, from the standpoint of computational efficiency, the adaptive calculation took 59 s and the 800-point equispaced case took 1,050 s—a factor of 17–18 more in CPU time. Hence, since the number of nodes used in the 800-point equispaced calculation and the adaptive calculation differs by a factor of 20, we see that determination of the adaptive grid is fairly inexpensive compared to the rest of the calculation.

Problem 2

The second problem we consider is a freely propagating, unsteady premixed flame with one-step chemistry (Peters and

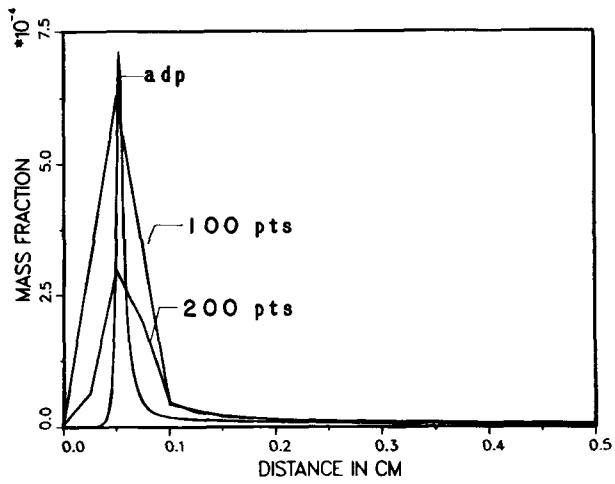

Figure 5. Comparison of HO_2 profile for adaptive calculation with 100- and 200-point equispaced results.

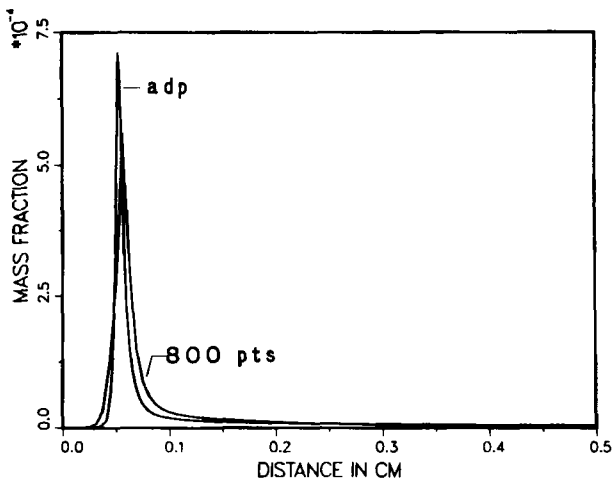

Figure 7. Comparison of HO_2 profile for adaptive calculation and 800-point equispaced result.

Warnatz, 1982). The governing equations are given by

$$\frac{\partial T}{\partial t} = \frac{\partial^2 T}{\partial x^2} + R, \tag{26}$$

$$\frac{\partial Y}{\partial t} = \frac{1}{Le}\frac{\partial^2 Y}{\partial x^2} - R, \tag{27}$$

where T is the normalized temperature and Y is the normalized mass fraction of the reactant. The normalized reaction rate R is written as

$$R = \frac{\beta^2}{2Le} Y \exp\left[-\frac{\beta(1-T)}{1-\alpha(1-T)}\right], \tag{28}$$

where Le is the Lewis number, β is a nondimensional activation energy, and α is a nondimensional heat release term. The initial conditions are given by

$$T = \exp(x), \quad x \le 0, \tag{29a}$$

$$Y = 1 - \exp(Lex), \quad x \le 0, \tag{29b}$$

and

$$T = 1, \quad x > 0, \tag{29c}$$

$$Y = 0, \quad x > 0, \tag{29d}$$

and the boundary conditions by

$$T = 0, \quad \text{as } x \to -\infty, \tag{30a}$$

$$Y = 1, \quad \text{as } x \to -\infty, \tag{30b}$$

and

$$\frac{dT}{dx} = 0, \quad \text{as } x \to \infty, \tag{30c}$$

$$\frac{dY}{dx} = 0, \quad \text{as } x \to \infty. \tag{30d}$$

We solve the problem for $\alpha = 0.8$, $\beta = 10.0$, and $Le = 1.0$. All of the calculations were carried out on the region $-50 \le x \le 50$.

Our numerical results reveal that the temperature and species profiles propagate as a function of time. In Figure 8 we illustrate calculated temperature profiles for the adaptive method with 75 points. (We also performed calculations with 100, 200, and 300 adaptive points but found that we first obtained a propagation velocity constant to two significant figures for 75 points). The profiles are shown for $t = 5.0$, 10.0, and 15.0. The points were chosen to equidistribute a weighted combination of the change in the solution and its gradient over consecutive mesh intervals. The adaptive method concentrated 40 of the 75 points in the region where $0.1 \le T \le 0.9$. We next performed the calculation with 75 equispaced points. The results are shown in Figure 9 for the same times as in Figure 8. We observe immediately the lack of resolution and the different location of the profiles compared to the adaptive calculation. It was not until we used 500 equispaced points, however, (Figure 10) that we obtained profiles with resolution and position comparable to the 75-point adaptive calculation.

Although the temperature is an important measurable quantity, the velocity of propagation is also a quantity of physical significance. It enables one to determine the time for a flame to propagate a fixed distance. This is important in a variety of combustion applications. In Table 1 we compare the velocity of propagation for several equispaced calculations (EQUI) and the 75-point adaptive calculation (ADP). Although the 500-point equispaced temperature profiles look comparable to the adaptive calculation, we find that the velocities of propagation still differ by about 10%. In fact, with as many as 1,000 points we are still several percent away from the adaptive velocity.

In Table 2 we compare the CPU times for the adaptive calculation and the 500- and 1,000-point equispaced calculations. Based upon the difference in the number of nodes, we again see that the adaptive calculation produces a considerable savings in CPU time over the equispaced method.

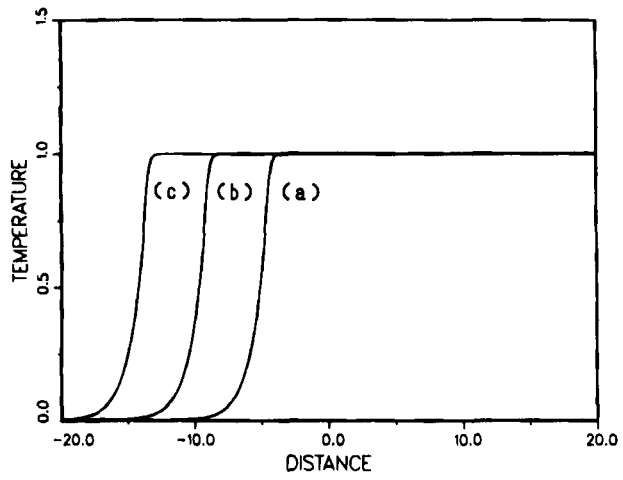

Figure 8. Temperature profiles for 75-point adaptive calculation.
a = 5.0, b = 10.0, c = 15.0

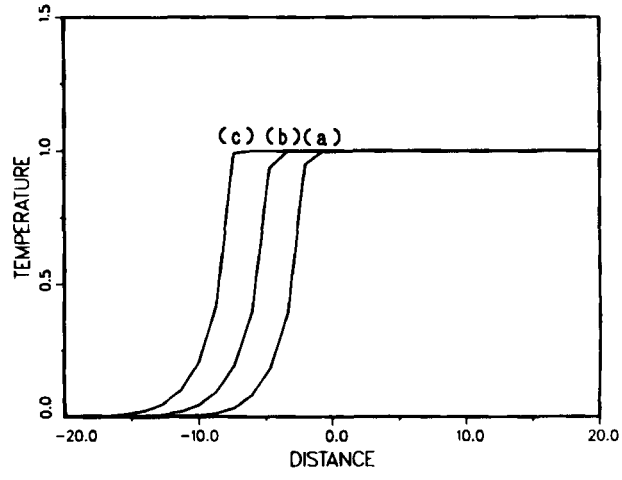

Figure 9. Temperature profiles for 75-point equispaced calculation.
a = 5.0, b = 10.0, c = 15.0

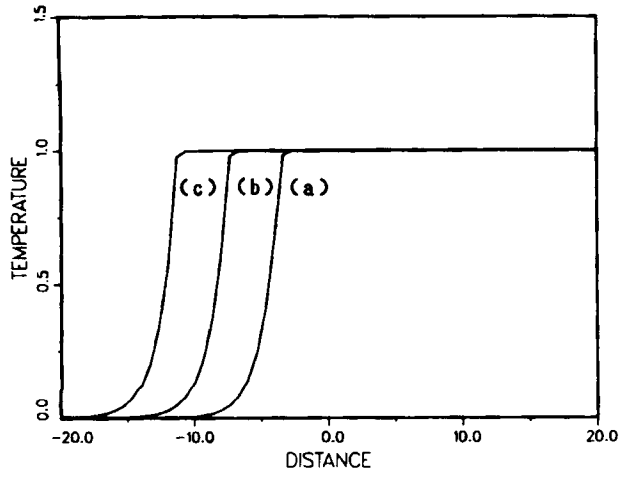

Figure 10. Temperature profiles for 500-point equispaced calculation.
a = 5.0, b = 10.0, c = 15.0

Summary

We have illustrated the use of adaptive numerical methods in the calculation of steady-state and time-dependent premixed flame structure. We have discussed the selection of grid points by equidistributing a positive weight function over consecutive mesh intervals. For steady state problems the equidistribution approach varies the number of points needed to satisfy some specified tolerance. In the time-dependent case, we apply an inverse interpolation algorithm with the equidistribution procedure applied to a fixed number of points. We have compared the use of equispaced and adaptive grids in the calculation of hydrogen-air flame speeds and in the resolution of the flame's intermediate species. We have also compared adaptive and equispaced propagation velocities for an unsteady freely propagating flame and we have observed the effects equispaced grids have on the resolution of the flame's temperature profile.

While the methods discussed in this paper are important for one-dimensional problems, their generalizations are essential in two-dimensional calculations. The savings in CPU time and central memory that can result from applying adaptive methods to two-dimensional problems can be the deciding factors as to whether a problem is computationally feasible.

Acknowledgment

This work was supported by the Office of Naval Research and the U.S. Department of Energy Office of Basic Energy Sciences.

Table 1. Velocity of Propagation for Freely Propagating Flame

Method	Nodes	Velocity
EQUI	75	−0.70
EQUI	150	−0.84
EQUI	250	−0.88
EQUI	500	−0.89
EQUI	1,000	−0.91
ADP	75	−0.96

EQUI, Equispaced calculations
ADP, Adaptive calculation

Table 2. CPU Time (in s) for Adaptive and Equispaced Methods

Method	Nodes	CPU
EQUI	500	245
EQUI	1,000	512
ADP	75	48

EQUI, Equispaced calculations
ADP, Adaptive calculation

Notation

a = start of computational domain
b = end of computational domain
C = equidistribution constant
c_p = constant pressure heat capacity of the mixture, J/kg · K
c_{pk} = constant pressure heat capacity of kth species, J/kg · K
f = nonlinear spatial function
F = residual form of discrete equations
g_1 = boundary conditions at $x = a$
g_2 = boundary conditions at $x = b$
h_j = jth mesh interval
h_k = specific enthalpy of kth species, J/kg
J = number of time levels
$J(V_k)$ = Jacobian matrix of kth Newton iterate
L = length of computational domain
Le = Lewis number
M = number of mesh intervals
$\dot{M}$ = mass flow rate, kg/m^2 · s
$\mathcal{M}$ = discrete mesh
N = number of dependent solution components
p = pressure, N/m^2
r = initial conditions
R = universal gas constant, J/mol · K
t = independent temporal coordinate
T = temperature, K
$\mathcal{T}$ = length of time integration
u = dependent solution components of continuous problem
$\tilde{u}$ = dependent solution components of semidiscrete problem
v = velocity, m/s
$V = (v_{ij})$ = discrete solution
V_k = diffusion velocity of kth species, m/s
w = weight function
W_k = molecular weight of kth species, kg/mol
$\bar{W}$ = mean molecular weight of mixture, kg/mol
x = independent spatial coordinate
Y_k = mass fraction of kth species

Greek letters

α = heat release
β = activation energy
δ = adaptive grid tolerance
γ = adaptive grid tolerance
ϵ_k = mass flux fraction of the kth species
λ = thermal conductivity, J/m · K · s
λ_k = kth damping parameter
τ^{n+1} = $(n+1)$st time step
$\dot{\omega}_k$ = molar rate of production of the kth species per unit volume, mol/m^3 · s

Literature cited

Ascher, U., J. Christiansen, and R. D. Russell, "COLSYS—A Collocation Code for Boundary Value Problems," *Proc. Conf. Working Codes for Boundary Value Problems in ODE's*, B. Childs et al., eds., Springer-Verlag, New York (1979).

Davis, S. F., and J. E. Flaherty, "An Adaptive Finite-Element Method for Initial-Boundary Value Problems for Partial Differential Equations," *SIAM J. Sci. Stat. Comput.*, **3**, 6 (1982).

Deuflhard, P., "A Modified Newton Method for the Solution of Ill-Con-

ditioned Systems of Nonlinear Equations with Application to Multiple Shooting," *Numer. Math.*, **22,** 289 (1974).
Dixon-Lewis, G., "Kinetic Mechanism, Structure, and Properties of Premixed Flames in Hydrogen-Oxygen-Nitrogen Mixtures," *Phil. Trans. Royal Soc. London,* **292,** 45 (1979).
Dwyer, H. A., R. J. Kee, and B. R. Sanders, "Adaptive Grid Methods for Problems in Fluid Mechanics and Heat Transfer," *AIAA J.*, **18,** 1205 (1980).
Dwyer, H. A., M. D. Smooke, and R. J. Kee, "Adaptive Gridding for Finite-Difference Solutions to Heat and Mass Transfer Problems," *Numerical Grid Generation,* J. F. Thompson, ed., Elsevier, New York (1982).
Harten, A., and J. M. Hyman, "A Self-Adjusting Grid for the Computation of Weak Solutions of Hyperbolic Conservation Laws," *J. Comp. Phys.*, **50,** 235 (1983).
Kautsky, J., and N. K. Nichols, "Equidistributing Meshes with Constraints," *SIAM J. Sci. Stat. Comput.*, **1,** 499 (1980).
Kee, R. J., J. A. Miller, and T. H. Jefferson, "CHEMKIN: A General-Purpose, Transportable, Fortran Chemical Kinetics Code Package," Sandia Nat. Labs. Rept. SAND80-8003 (1980).
Kee, R. J., J. Warnatz, and J. A. Miller, "A Fortran Computer Code Package for the Evaluation of Gas-Phase Viscosities, Conductivities, and Diffusion Coefficients," Sandia Nat. Labs. Rept. SAND83-8209 (1983).
Larrouturou, B., "Unsteady One-Dimensional Flame Propagation Using Adaptive Grids," *Symp. Numerical Simulation of Combustion Phenomena,* INRIA, Springer-Verlag, (1985).
Miller, K., and R. Miller, "Moving Finite Elements. I," *SIAM J. Numer. Anal.*, **18,** 1019 (1981).
Miller, J. A., R. E. Mitchell, M. D. Smooke, and R. J. Kee, "Toward a Comprehensive Chemical Kinetic Mechanism for the Oxidation of Acetylene: Comparison of Model Predictions with Results from Flame and Shock Tube Experiments," *19th Int. Symp. Combustion,* Reinhold, New York, 181 (1982).
Miller, J. A., M. D. Smooke, R. M. Green, and R. J. Kee, "Kinetic Modeling of the Oxidation of Ammonia in Flames," *Comb. Sci. Tech.*, **34,** 149 (1983).
Pearson, C. E., "A Numerical Method for Ordinary Differential Equations of Boundary-Layer Type," *J. Math. Phys.*, **47,** 134 (1968).
Pereyra, V., and E. G. Sewell, "Mesh Selection for Discrete Solution of Boundary Value Problems in Ordinary Differential Equations," *Numer. Math.*, **23,** 261 (1975).
Peters, N., and J. Warnatz, eds., *Numerical Methods in Laminar Flame Propagation,* Vieweg, Wiesbaden (1982).
Russell, R. D., "Mesh Selection Methods," *Proc. Conf. Working Codes for Boundary Value Problems in ODE's,* B. Childs et al., eds., Springer-Verlag, New York (1979).
Sermange, M., "Mathematical and Numerical Aspects of One-Dimensional Laminar Flame Simulation," INRIA Rept. No. 446 (1985).
Smooke, M. D., "Solution of Burner-Stabilized Premixed Laminar Flames by Boundary Value Methods," *J. Comp. Phys.*, **48,** 72 (1982).
———, "An Error Estimate for the Modified Newton Method with Applications to the Solution of Nonlinear Two-Point Boundary Value Problems," *J. Opt. Theory Appl.*, **39,** 489 (1983).
Smooke, M. D., and M. L. Koszykowski, "Two-Dimensional Fully Adaptive Solutions of Solid-Solid Alloying Reactions," *J. Comp. Phys.* (1986).
Smooke, M. D., and M. L. Koszykowski, "Fully Adaptive Solutions of One-Dimensional Mixed Initial-Boundary Value Problems with Applications to Unstable Problems in Combustion," *SIAM J Sci. and Stat. Comp.*, **7,** 301 (1986).
Smooke, M. D., J. A. Miller, and R. J. Kee, "Determination of Adiabatic Flame Speeds by Boundary Value Methods," *Comb. Sci. and Tech.*, **34,** 79 (1983).
———, "Solution of Premixed and Counterflow Diffusion Flame Problems by Adaptive Boundary Value Methods," *Numerical Boundary Value ODE's,* U. M. Ascher and R. D. Russell, eds., Birkhauser, Cambridge (1985).
Tscharnuter, W. M., and K. H. Winkler, "A Method for Computing Self-gravitating Gas Flows with Radiation," *Compt. Phys. Comm.*, **18,** 171 (1979).
White, A. B., "On Selection of Equidistributing Meshes for Two-Point Boundary Value Problems," *SIAM J. Numer. Anal.*, **16,** 472 (1979).
———, "On the Numerical Solution of Initial/Boundary-Value Problems in One Space Dimension," *SIAM J. Numer. Anal.*, **19,** 683 (1982).

Manuscript received Apr. 30, 1985, and revision received Feb. 26, 1986.

Appendix

Reaction mechanism rate coefficients in the form $k_f = AT^{\beta} \exp(-E_0/RT)$. Units are moles, cubic centimeters, seconds, Kelvins, and calories/mole.

Reaction	A	β	E
1. $H_2 + O_2 \rightleftharpoons 2OH$	1.70 E + 13	0.000	47,780
2. $OH + H_2 \rightleftharpoons H_2O + H$	1.17 E + 09	1.300	3,626
3. $H + O_2 \rightleftharpoons OH + O$	5.13 E + 16	−0.816	16,507
4. $O + H_2 \rightleftharpoons OH + H$	1.80 E + 10	1.000	8,826
5. $H + O_2 + M \rightleftharpoons HO_2 + M^*$	2.10 E + 18	−1.000	0
6. $H + O_2 + O_2 \rightleftharpoons HO_2 + O_2$	6.70 E + 19	−1.420	0
7. $H + O_2 + N_2 \rightleftharpoons HO_2 + N_2$	6.70 E + 19	−1.420	0
8. $OH + HO_2 \rightleftharpoons H_2O + O_2$	5.00 E + 13	0.000	1,000
9. $H + HO_2 \rightleftharpoons 2OH$	2.50 E + 14	0.000	1,900
10. $O + HO_2 \rightleftharpoons O_2 + OH$	4.80 E + 13	0.000	1,000
11. $2OH \rightleftharpoons O + H_2O$	6.00 E + 08	1.300	0
12. $H_2 + M \rightleftharpoons H + H + M^{**}$	2.23 E + 12	0.500	92,600
13. $O_2 + M \rightleftharpoons O + O + M$	1.85 E + 11	0.500	95,560
14. $H + OH + M \rightleftharpoons H_2O + M^{\dagger}$	7.50 E + 23	−2.600	0
15. $H + HO_2 \rightleftharpoons H_2O_2$	2.50 E + 13	0.000	700
16. $HO_2 + HO_2 \rightleftharpoons H_2O_2 + O_2$	2.00 E + 12	0.000	0
17. $H_2O_2 + M \rightleftharpoons OH + OH + M$	1.30 E + 17	0.000	45,500
18. $H_2O_2 + H \rightleftharpoons HO_2 + H_2$	1.60 E + 12	0.000	3,800
19. $H_2O_2 + OH \rightleftharpoons H_2O + HO_2$	1.00 E + 13	0.000	1,800

*Third-body efficiencies: $k_5(H_2O) = 21k_5(Ar)$, $k_5(H_2) = 3.3k_5(Ar)$, $k_5(N_2) = k_5(O_2) = 0$.
**Third-body efficiencies: $k_{12}(H_2O) = 6k_{12}(Ar)$, $k_{12}(H) = 2k_{12}(Ar)$, $k_{12}(H_2) = 3k_{12}(Ar)$.
†Third-body efficiency: $k_{14}(H_2O) = 20k_{14}(Ar)$.